Meteoritics & Planetary Science 37, 1165–1172 (2002)
Available online at http://www.uark.edu/meteor

The sodium tail of Mercury

A. E. POTTER[1]*, R. M. KILLEN[2] AND T. H. MORGAN[3]

[1]National Solar Observatory, P.O. Box 26732, 950 North Cherry Avenue, Tucson, Arizona 85726-6732, USA
[2]Southwest Research Institute, 6220 Culebra Road, San Antonio, Texas 78228-0510, USA
[3]NASA Headquarters, 300 E Street SW, Washington, D.C. 20546-0001, USA
*Correspondence author's e-mail address: apotter@noao.edu

(Received 2001 December 24; accepted in revised form 2002 March 20)
(Presented at the Workshop on Mercury, The Field Museum, Chicago, Illinois, 2001 October 4–5)

Abstract–Mercury is difficult to observe because it is so close to the Sun. However, when the angle of the ecliptic is near maximum in the northern hemisphere, and Mercury is near its greatest eastern elongation, it can be seen against the western sky for about a half hour after sunset. During these times, we were able to map sodium D_2 emission streaming from the planet, forming a long comet-like tail. On 2001 May 26 (U.T.) we mapped the tail downstream to a distance of ~40 000 km. Sodium velocities in the tail increased to ~11 km s^{-1} at 40 000 km as the result of radiation pressure acceleration. On 2000 June 5 (U.T.) we mapped the cross-sectional extent of the tail at a distance of ~17 500 km downstream. At this distance, the half-power full-width of the emission was ~20 000 km. We estimated the transverse velocity of sodium in the tail to range from 2 to 4 km s^{-1}. The velocities we observed imply source velocities from the planet surface of the order of 5 km s^{-1}, or 4 eV. Particle sputtering is a likely candidate for production of sodium atoms at these velocities. The total flux of sodium in the tail was ~1 × 10^{23} atoms s^{-1}, which corresponds to 1 to 10% of the estimated total production rate of sodium on the planet.

INTRODUCTION

Solar radiation acceleration on sodium atoms in the atmosphere of Mercury varies with position in the orbit, depending on distance from the Sun and the radial velocity of Mercury. The maximum acceleration of ~200 cm s^{-2} (54% of surface gravity) occurs at true anomaly angles near 64° and 300°, and the minimum acceleration of ~12 cm s^{-2} occurs at aphelion, true anomaly angle = 180°. Ip (1986), Smyth (1986) and Smyth and Marconi (1995) have modeled the effect of radiation acceleration on the trajectories of sodium atoms emitted from the surface at various velocities. For the minimum value of solar radiation acceleration, the shape of the sodium atmosphere is essentially the same as it would be for solar radiation acceleration of zero, producing a "normal" spherically symmetric atmosphere. However, for the maximum value of the solar radiation acceleration, the atmosphere is severely depressed at the subsolar point, and for sodium atoms leaving the surface at velocities >2 km s^{-1}, the atoms can escape the planet to form a long comet-like neutral sodium tail. If it could be observed, the morphology of the sodium tail behind the planet could be used to infer the ejection conditions, and thus help to understand the source processes for sodium on Mercury.

The spatial character and density of the sodium atmosphere and tail will change with the position of Mercury in orbit as a consequence of the changes of radiation acceleration. But in addition to this effect, there is evidence that space weather in the vicinity of Mercury can also produce substantial changes in the sodium atmosphere as a result of changes in sodium production processes (Killen *et al.*, 2001). These changes would also be reflected in the morphology of the sodium tail.

Previous efforts to detect the sodium tail by means of observations done during daylight hours have been only partly successful because scattered sunlight obscured the weak sodium emissions in the tail (Potter and Morgan, 1997). However, at greatest eastern elongation for a few months around the March equinox in the northern hemisphere, Mercury can be seen as an evening star for about a half-hour. At this time, the intensity of scattered sunlight is low enough that sodium emissions as low as 500 R (rayleighs) can be detected. The time available for observation is limited to ~30 min, but during that time we were able to map the general shape and extent of the sodium tail of Mercury.

OBSERVATIONS

We used the 1.6 m McMath–Pierce Solar Telescope at the National Solar Observatory, Kitt Peak, Arizona, USA to observe Mercury after sunset against a dark sky on the evening of 2000 June 4 and again on the evening of 2001 May 25,

Prelude preprint MS#4716

TABLE 1. Planetary configurations at the times of observations.

Date and time (U.T.)	Phase angle (°)	Heliocentric distance (AU)	Radial velocity (km s^{-1})	Solar radiation acceleration (cm s^{-2})
0300 2000 June 5	93.0	0.4051725	9.15249	168
0300 2001 May 26	116.1	0.4208615	8.19359	140

corresponding to universal time dates of June 5 and May 26, respectively. The properties of Mercury at these times are listed in Table 1. We used a 10 × 10 arcsec image slicer to view Mercury and the tail region. Eight to 10 observations at various positions downstream of Mercury were possible during the 30–40 min that Mercury could be observed. The image slicer dissected the field of view into ten 1 arcsec wide slices that were placed end-to-end on the entrance slit of the McMath–Pierce Stellar Spectrograph. The resulting echelle spectra were recorded on an 800 × 800 element Texas Instruments charge-coupled device (CCD) at a resolution of ~150 000. At this resolution, sodium emission from terrestrial twilight glow is clearly separated from Mercury sodium emission. This is shown in Fig. 1, which displays a spectrum of the sky at a distance of ~50 arcsec downstream (eastward) from Mercury. As a result of the velocity of Mercury relative to Earth, the sodium emission from Mercury is shifted 0.61 Å blueward (to shorter wavelengths) from the sodium emission from the twilight glow.

The spatial-spectral images were analyzed to yield 10 × 10 arcsec images of the sodium D emission with 1 arcsec square pixels. We used the peak reflectance signal from the surface of Mercury as the calibration signal as previously described (Potter *et al.*, 1999). It was necessary to use the last image obtained with Mercury in the field of view to calibrate all of the spectral data obtained when Mercury was out of the field of view. The peak intensities seen in the last image were ~3000 kR for observations on 2000 June 4, and 6000 kR for observations on 2001 May 25. These values are in general agreement with previous observations of Mercury sodium (Sprague *et al.*, 1997; Potter *et al.*, 1999, and references therein). These later spectra were observed at larger air masses than the calibration spectrum, so that an extinction correction was necessary for these spectra. For this, we used the average extinction corrections recommended by Green (1992).

DOWNSTREAM EMISSION PROFILE OF THE TAIL

Observations on the evening of 2001 May 25 (0300 U.T. May 26) were directed towards determining the downstream profile of the emission. Ten exposures were made, with integration times varying from 30 s for planet Mercury in the field of view to 5 min for the exposure farthest downstream from Mercury, at 60 arcsec angular distance.

The resulting sodium D_2 images are shown in Fig. 2. The intensity of the sodium emission ranges over 3 orders of magnitude, so that it is necessary to use a logarithmic scale to display the data. For this figure, the angular distances have been converted to line-of-sight geometric distances. The figure shows that sodium emission can be detected downstream for ~40 000 km. Sodium is seen to be streaming away from the poles at angles >45° to the tail direction, which suggests that some sodium is emitted from Mercury at high latitudes. Killen *et al.* (2001) have shown that ion sputtering will result from ions entering the cusp regions at high latitudes. Our observation that sodium appears to be ejected from the planet at high latitudes is consistent with this. In order to quantify the information seen in the tail images, we averaged each 10-element column. Each average value provided one point in a plot of emission intensity *vs.* distance. The line-of-sight distance was converted to heliocentric distance by dividing by cosine of the phase angle. Intensities were corrected for extinction as described above. The resulting semilog plot is shown in Fig. 3. After ~15 000 km from Mercury, the sodium

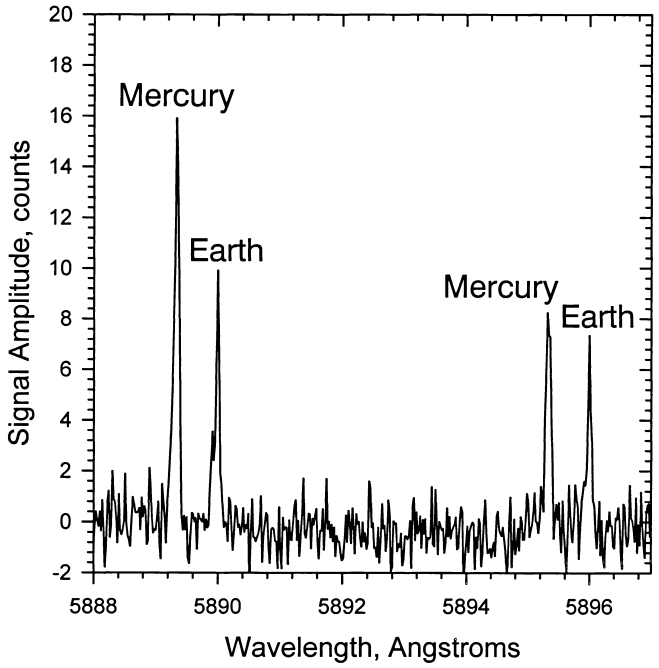

FIG. 1. The spectrum of sodium D lines at a location 33 000 km downstream of Mercury on 0300 U.T. 2001 May 26. The sodium lines from Mercury are shifted 0.62 Å to shorter wavelengths from the terrestrial twilight glow lines because of the velocity of Mercury relative to the Earth.

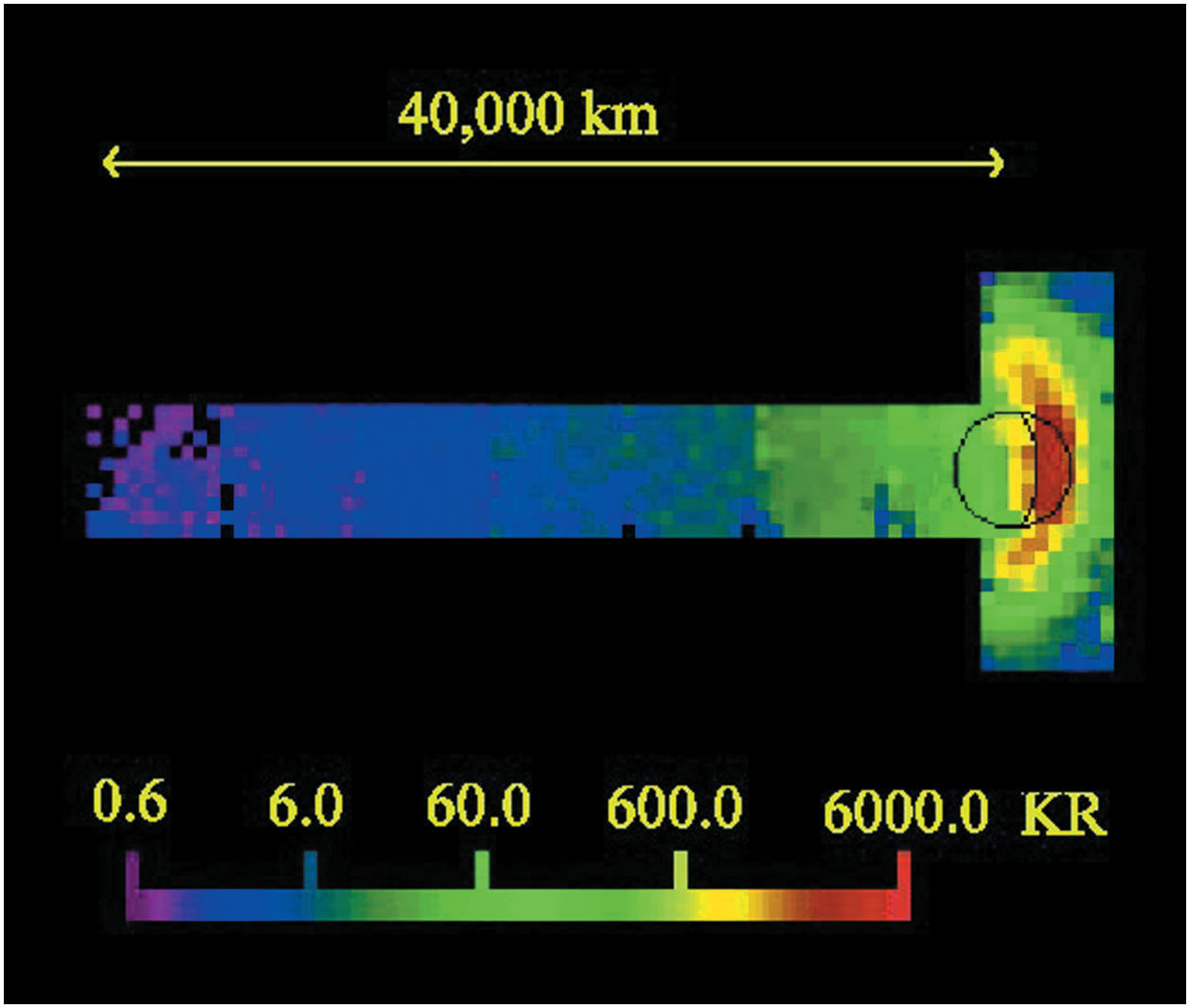

FIG. 2. Images of the sodium D_2 emission intensity in kilorayleighs (kR) downstream (anti-sunward) of Mercury at 0300 U.T. 2001 May 26. Each square represents an observation with the 10 × 10 arcsec image slicer, and represents an area 5100 km on a side. The emission intensity varies over 4 orders of magnitude, from ~0.6 to 6000 kR. These observations were tailored towards measurement of the downstream profile of the tail along its axis. West is on the right, and south is at the top of the figure.

emission intensity decreased logarithmically with increasing distance. The slope of the line was 0.031 $\log_{10}$ kR $(10^3$ km$)^{-1}$. In order to interpret the emission intensities in terms of atom densities, we need to know the g values (atoms photons^{-1} s^{-1}) at every point in the tail. The g values change as sodium is accelerated to higher velocities by radiation pressure acceleration. Consequently, it is necessary to know the velocity of the sodium atoms at each point in the tail to convert emission intensities to atom densities. We determined the sodium velocities in the tail by measurement of the Doppler shift of the lines.

VELOCITIES IN THE TAIL

In order to measure the Doppler shifts of the sodium D_2 emission lines in the tail, we averaged all 100 spectra in each of the slicer images to provide one high signal-to-noise spectrum at each slicer image position. The centroid of the emission line in this spectrum was measured. The shift of the centroid position from the rest position on Mercury was converted to line-of-sight velocities of the atoms relative to Mercury. These velocities were converted to heliocentric velocities by dividing by the sine of the phase angle. Figure 4 shows a plot of heliocentric sodium velocities relative to Mercury plotted against heliocentric distance. The velocity does not change much up to ~15 000 km, but at greater distances the velocity increases more or less linearly up to ~11 km s^{-1}.

To compare the sodium velocities with theoretical expectations, we calculated what the velocities should be at different distances from Mercury by a stepwise integration, taking into account the changes in radiation pressure acceleration as the velocity of the sodium atoms increases. The radiation pressure depends on the heliocentric velocity of the

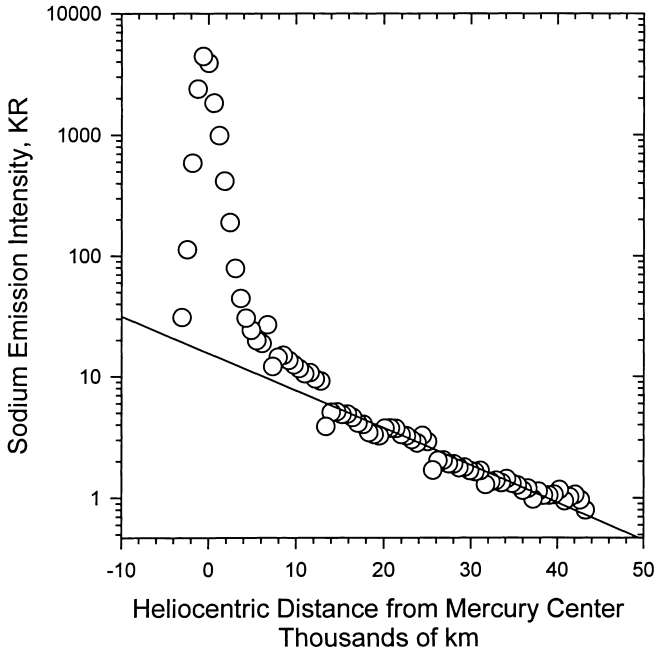

FIG. 3. The emission intensity in kilorayleighs (kR) along the axis of the Mercury sodium tail at 0300 U.T. 2001 May 26. The line-of-sight distances have been converted to heliocentric distances. The semilogarithmic plot becomes linear at distances greater than ~15 000 km, with a slope of 0.031 $\log_{10}$ kR $(10^3$ km$)^{-1}$.

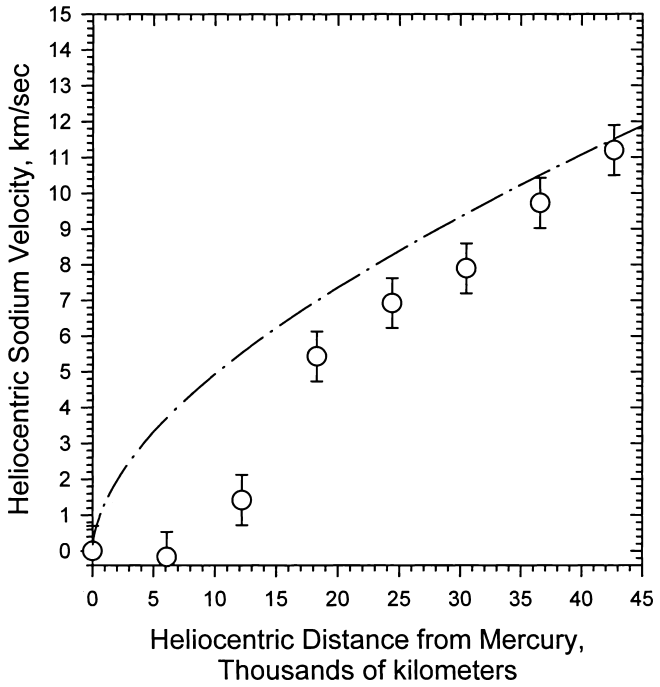

FIG. 4. Heliocentric velocities of sodium atoms in the Mercury tail at 0300 U.T. 2001 May 26. Velocities are relative to Mercury. The line that is plotted is the best theoretical fit we could get to the data, and was calculated assuming that sodium was ejected sunward from Mercury with a velocity of 2.5 km s^{-1}. Up to ~15 000 km from Mercury, the observed velocities are considerably less than the computed velocities. Most of this difference is probably the result of strong emissions from sodium at rest relative to the planet, which have been scattered into the field of view.

sodium atom, since the solar flux responsible for the radiation pressure varies by almost a factor of 20 between the bottom of the Fraunhofer line and the nearby continuum. On the date of these observations, the heliocentric velocity of sodium at rest on Mercury was 9.15 km s^{-1}. As a consequence, the sodium atoms see a solar spectrum that is shifted ~180 mÅ redward. Radiation pressure acceleration will increase the antisunward velocity of the sodium, resulting in a further apparent redward shift of the solar spectrum, and a further increase in acceleration and velocity. For sodium atoms emitted at exactly the radial velocity of Mercury (*i.e.*, at rest relative to Mercury), the predicted velocities were all 2–3 km s^{-1} higher than the observed data. A better fit was obtained using an initial antisunward ejection velocity of 2.5 km s^{-1}, which produced the line plotted in Fig. 4. Higher ejection velocities produced little improvement in the fit. The predicted velocities close to Mercury, at distances less than ~15 000 km, are larger than the observed velocities, which increase very little with downstream distance in this region. Sodium emissions seen at these relatively close-in distances are probably dominated by unshifted emissions from the bright planet scattered into the field of view.

SODIUM DENSITIES IN THE TAIL

Knowing the velocity at different distances in the tail, it is possible to estimate the column densities in the tail, taking into account the changes of g factor that result from the changing sodium velocity. The computed column densities in the tail are plotted in Fig. 5. In the linear portion of the semilog plot, the slope was 0.036 $\log_{10}$ atoms cm^{-2} $(10^3$ km$)^{-1}$. The slope of the line is affected by two factors. One is the loss of sodium by photoionization. The other is transverse velocity of sodium in the tail, which results in a lateral spreading of the tail causing the intensity of emission along the centerline to decrease.

CROSS-SECTIONAL PROFILE OF THE TAIL

Observations of the sodium tail were also accomplished on the evening of 2000 June 4 (0300 U.T. June 5). Eleven images were measured, distributed both downstream and at right angles to the tail, as shown in Fig. 6, which displays the measured intensities on a logarithmic scale. Figure 7 shows a plot of centerline sodium D_2 emission intensity plotted against heliocentric distance. Results are similar to those from the 2001 May 26 U.T. observations. The semilogarithmic plot is linear beyond a distance of ~15 000 km, with a slope of 0.030 $\log_{10}$ kR $(10^3$ km$)^{-1}$, close to the slope observed on 2001 May 26. As before, in order to convert the emission intensities into atom densities, we need to know the sodium velocities. However, the Mercury phase angle on this date was 93.8° so

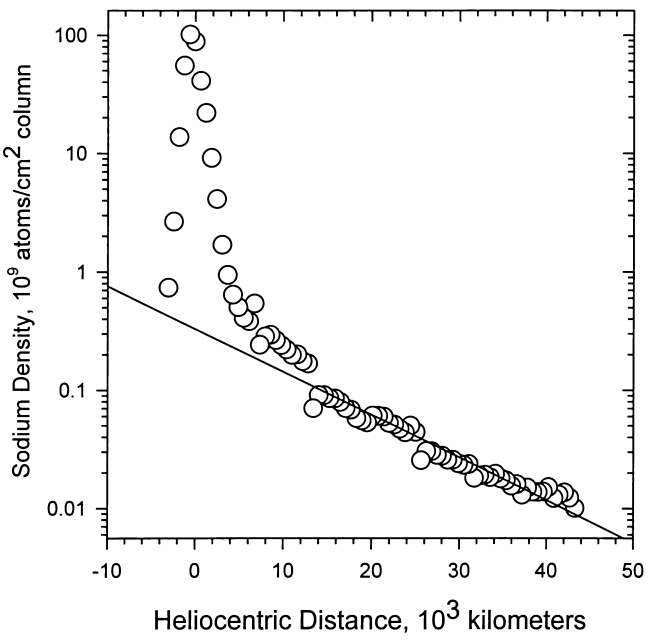

FIG. 5. The sodium atom column density, atoms cm^{-2} column in the Mercury tail at 0300 U.T. 2001 May 26. Heliocentric velocities from the theoretical fit to the observed velocities in the tail were used to compute values of g (atoms $photon^{-1}$ s^{-1}) at various heliocentric distances down the tail. The linear portion of the semilog plot begins between 10 000 and 15 000 km, and has a slope of 0.036 $\log_{10}$ atoms cm^{-2} $(10^3$ km$)^{-1}$.

that the tail was viewed at a near-right angle of 86.2°. This angle precluded the accurate measurement of heliocentric Doppler shifts in the sodium emission line caused by solar radiation pressure. Consequently, we calculated the sodium velocities in the tail using the procedure outlined above, assuming, as before, that the sodium was ejected from the planet at a velocity of 2.5 km s^{-1} towards the Sun. We used these velocities to calculate the g factors along the tail. The resulting sodium densities are plotted in Fig. 8. The slope of the linear part of the semilogarithmic plot was 0.038 $\log_{10}$ atoms cm^{-2} $(10^3$ km$)^{-1}$.

The 2000 June 4 data set also allows us to map the cross-section of the sodium tail, since at ~16 700 km downstream, we have four slicer observations that span the entire width of the tail. We have already calculated the g factors needed to convert the emission intensities to atom densities. Figure 9 shows a plot of sodium column density normal to the axis of the tail at a downstream heliocentric distance of ~16 700 km. At this distance, the tail has expanded to a diameter of nearly 40 000 km, with a half-power full width of ~20 000 km. We can use these data to calculate the transverse velocities in the tail, provided we know the time required for sodium emitted from Mercury to reach this location. As previously noted, we do not have measured velocities for this date, but if we use the calculated velocities, we find that the time elapsed for the sodium to reach a distance of 16 700 km to be ~5000 s. The full-width half-power of the tail cross-section is ~20 000 km. In order for a sodium atom to travel outwards from the centerline to the half-power point at 10 000 km, its velocity must be ~2 km s^{-1}. Atoms which reach the edge of the tail must have had transverse velocities of ~4 km s^{-1}.

DISCUSSION

The atom column density in the sodium tail can be described approximately by

$$N = \frac{Q}{lV_h}\exp(-t/r^2\tau) \tag{1}$$

where N is the number of atoms per unit area, Q is the source rate, l is the width of the tail, V_h is the velocity of atoms in the tail, t is time elapsed since the sodium atoms were produced, r is the distance from the Sun in AU, and τ is the lifetime of sodium atoms against photoionization at 1 AU.

Noting that the width of the tail $l = 2V_t t$, where V_t is the transverse velocity in the tail (assumed to be constant), and that the downstream distance D in the tail is defined by $V_h t$, we find that

$$\frac{d\ln N}{dD} = -\frac{1}{D} - \frac{1}{V_h r^2 \tau} \tag{2}$$

The values of $d\ln N/dD$ found in the linear part of the semilog plots of sodium column density *vs.* distance down the tail ranged from 0.83 $(10^3$ km$)^{-1}$ on 2001 May 26 to 0.088 $(10^3$ km$)^{-1}$ on 2000 June 5 (the $\log_{10}$ values quoted previously have been converted here to $\log_e$ values). There are several values in the literature for the solar photoionization lifetime of sodium atoms: Carlson *et al.* (1975) proposed 5.46×10^4 s^{-1}, Hunten *et al.* (1988) proposed 8.00×10^4 s^{-1}, and Huebner *et al.* (1992) proposed a value of 16.9×10^4 s^{-1} (all at 1 AU). We can use these values to predict the slopes of the semilogarithmic plots of sodium column density *vs.* distance. The average velocity of sodium atoms in the linear regions of the plots is ~7 km s^{-1}, as derived from the Doppler shift data. In the linear regions of the semilogarithmic plots, the lateral spreading term $(1/D)$ has an average value of ~0.03 $(10^3$ km$)^{-1}$. Table 2 shows a comparison between slopes observed and those calculated using the literature values of photoionization lifetime quoted above. The observed slopes are about a factor of 2 larger than the predicted slopes—the sodium density decreases faster with distance than predicted. One possible explanation might be that the observations did not follow the centerline of the tail, but veered off towards the edge of the tail at increasing distances from the planet. Since the sodium density decreases away from the centerline, this would cause the observed density to decrease more rapidly than if the observations had followed the centerline. Another possible explanation might be that the extinction correction was underestimated. Future observations of the tail will be designed to minimize these possible sources of error.

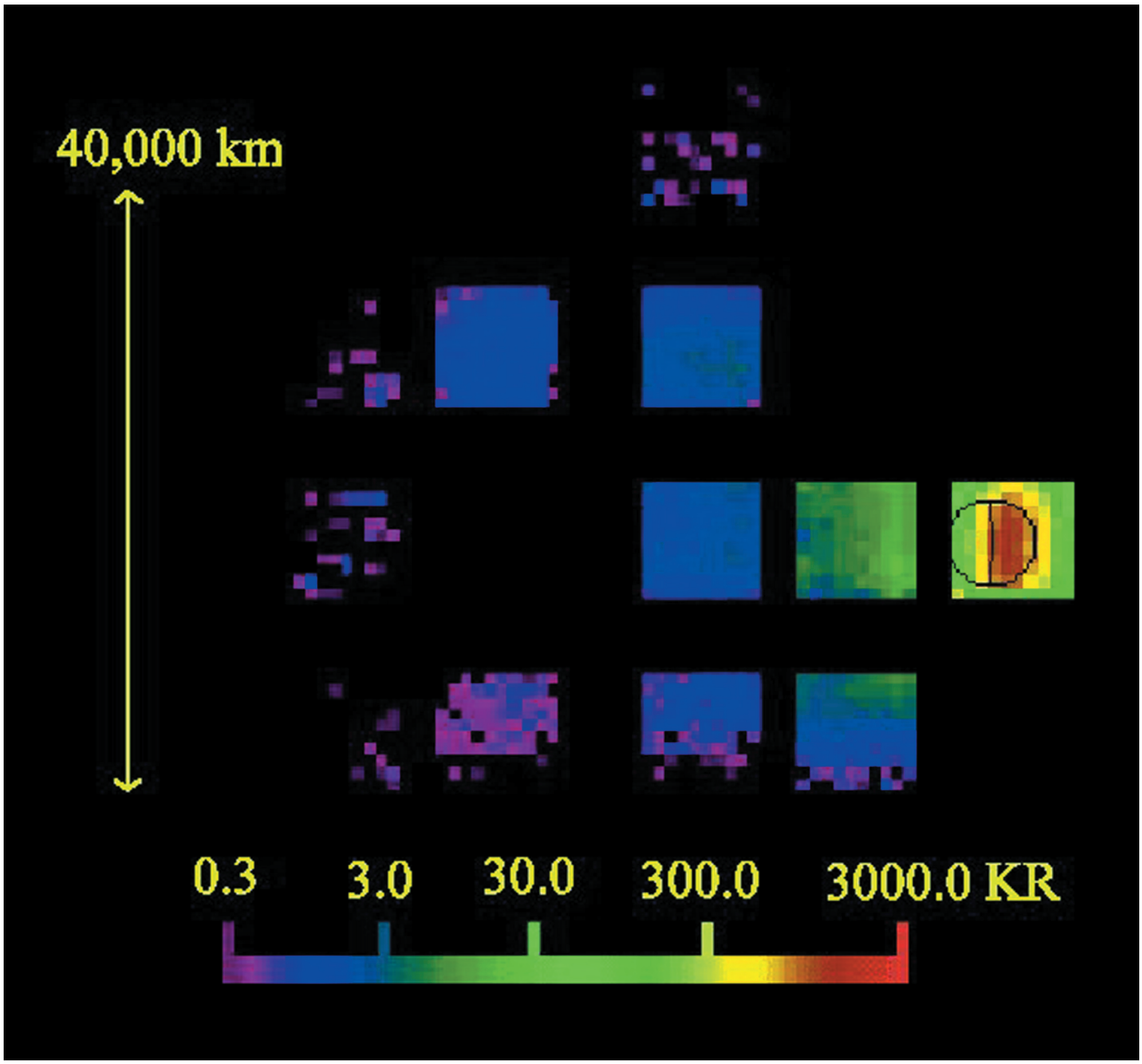

FIG. 6. Images of the sodium D_2 emission downstream (anti-sunward) of Mercury at 0300 U.T. 2000 June 5. Each square represents an observation with the 10 × 10 arcsec image slicer, and represents an area 5900 km on a side. The emission intensity varies over 4 orders of magnitude, from ~0.3 to 3000 kR. These observations were tailored towards measurement of the cross-section of the tail. West is on the right, and south is at the top of the figure.

TABLE 2. Comparison of observed and calculated decay rates for sodium density in the tail.

Date and time (U.T.)	Observed slope This study $(10^3$ km$)^{-1}$	Predicted slope Carlson *et al.* (1975) $(10^3$ km$)^{-1}$	Predicted slope Hunten *et al.* (1988) $(10^3$ km$)^{-1}$	Predicted slope Huebner *et al.* (1992) $(10^3$ km$)^{-1}$
0300 2000 June 5	–0.088	–0.046	–0.041	–0.035
0300 2001 May 26	–0.083	–0.044	–0.040	–0.035

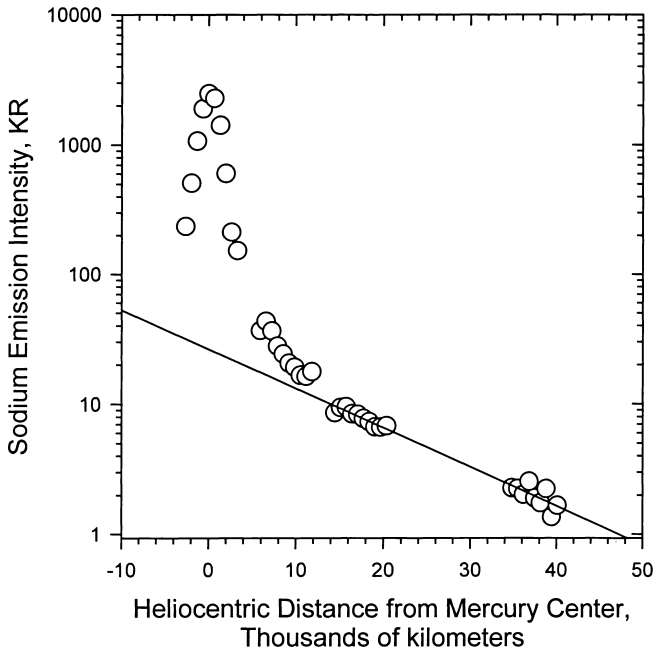

FIG. 7. The emission intensity in kilorayleighs (kR) along the axis of the Mercury sodium tail at 0300 U.T. 2000 June 5. The line-of-sight distances shown in Fig. 2 have been converted to heliocentric distances. Although there were only two 10 × 10 slicer observations along the tail axis, the slope of the linear portion of the plot is similar to that observed from the 2001 May 26 data. The semilogarithmic plot becomes linear at distances greater than ~15 000 km, with a slope of 0.030 $\log_{10}$ kR $(10^3$ km$)^{-1}$.

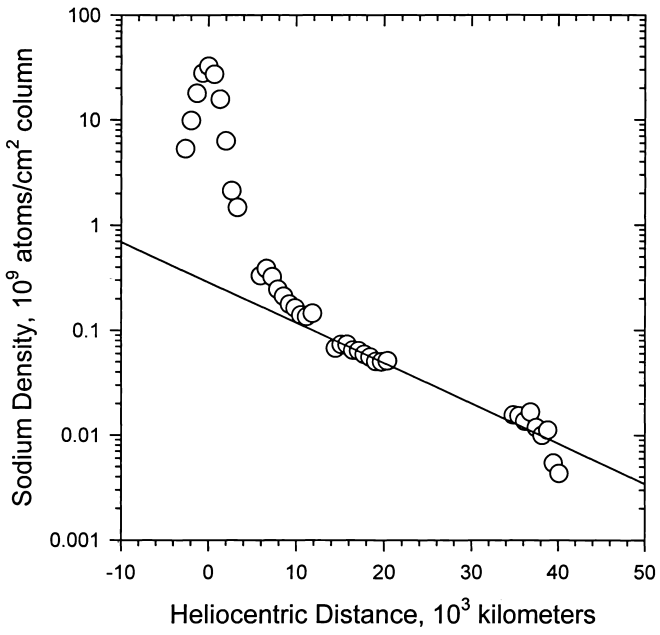

FIG. 8. The sodium atom density, atoms cm^{-2} column in the Mercury tail at 0300 U.T. 2001 May 26. Heliocentric velocities from the theoretical fit to the observed velocities in the tail were used to compute values of g (atoms $photon^{-1}$ s^{-1}) at various heliocentric distances down the tail. The linear portion of the semilog plot begins between 10 000 and 15 000 km, and has a slope of 0.038 $\log_{10}$ atoms cm^{-2} $(10^3$ km$)^{-1}$.

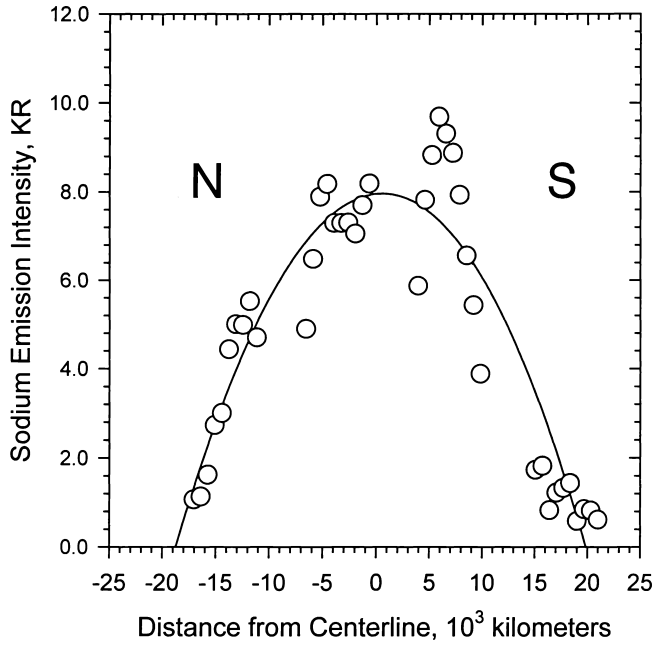

FIG. 9. This plot shows the cross-section of sodium column density, atoms cm^{-2} column, in the tail at a distance of 16 700 km downstream from Mercury. The downstream sodium velocities needed to convert the emission intensities to atom densities were calculated theoretically, as for the plot shown in Fig. 4. While a parabolic curve has been drawn through the data, it should be noted that the distribution is actually asymmetric, with a higher intensity on the southern side than on the northern side. This suggests that the axis of symmetry of the tail was tilted in a southern direction for these observations.

The fact that an extended sodium tail can be detected is evidence that sodium is produced with sufficient energy to escape the planet. Ip (1986), Smyth (1986) and Smyth and Marconi (1995) found that sodium source velocities of 2 km s^{-1} should be sufficient for sodium to escape from the planet under the influence of the maximum solar radiation acceleration. Radiation acceleration of sodium atoms on 2000 June 5 (U.T.) was 45% of surface gravity, and on 2001 May 26 (U.T.) was 40% of surface gravity. In both cases, the escape velocity of sodium is reduced from the nominal value of 4.25 to ~2.5 km s^{-1}. The transverse velocities of 2–4 km s^{-1} and the need to assign an antisunward velocity of sodium leaving the planet of 2.5 km s^{-1}, suggests that the sodium left the surface of the planet with velocities of the order of 5 km s^{-1}, or ~4 eV. Particle sputtering is a likely candidate for production of sodium atoms at these energies. The relatively high sodium velocity at right angles to the Mercury–Sun line (2–4 km s^{-1}) suggests that much of the sodium is generated at high latitudes, rather than near the equator.

An important question is what fraction of the sodium produced on Mercury enters the tail? We can use the tail cross-section data from 2000 June 5 (U.T.) to estimate the total flux of sodium in the tail. The line plot of atoms cm^{-2} was integrated from side to side across the tail region, yielding a total sodium amount of 1.6×10^{17} atoms cm^{-1}. We do not have velocity

measurements for this set of data because the tail was oriented almost exactly at right angles to the line of sight. However, if we use the calculated velocities, we find a velocity of 6.6 km s^{-1} at 16 700 km downstream from Mercury. Multiplying this velocity by the total sodium yields a total flux of sodium atoms from the planet of 1.1×10^{23} atoms s^{-1}.

In order to determine what fraction of total sodium production is lost to the tail, we must know the rate of sodium production from the surface of Mercury. However, this value is not well defined. Killen and Morgan (1993) suggest a surface source rate of 10^7 atoms cm^{-2} s^{-1} which corresponds to a total production rate of 3.8×10^{24} atoms s^{-1} for a hemispherical area of 3.75×10^{17} cm^2.

Smyth and Marconi (1995) gave an estimate of 10^{25} atoms s^{-1}. Ip (1990) proposed a rate of $(5–9) \times 10^{24}$ atoms s^{-1}, and Hunten and Sprague (1997) proposed a surface source rate of $(3.6 \pm 2.4) \times 10^6$ atoms cm^{-2} s^{-1}, which corresponds to a total production rate of $(1.35 \pm 0.9) \times 10^{24}$ atoms s^{-1}. From these values, it appears that the sodium in the tails represented a fraction somewhere between 1 and 10% of the total sodium produced on Mercury.

These results support the analysis by McGrath *et al.* (1986), who concluded that ion sputtering should be an important loss mechanism for sodium atoms. The high velocities of the sputtered atoms would lead to their escape from the planet. It could produce loss rates of 10^5 to 10^6 atoms cm^{-2} s^{-1}. These would correspond to total loss rates of $\sim 3.8 \times 10^{22}$ to 10^{23} atoms s^{-1}, which are in order-of-magnitude agreement with the observed loss rates. However, McGrath *et al.* (1986) pointed out that ion sputtering could not account for all of the observed sodium. The bulk of sodium on Mercury displays translational temperatures near 1000 K (Killen *et al.*, 1999), which corresponds roughly to the temperature expected from photon sputtering of sodium (Madey *et al.*, 1998). Consequently, it seems likely that much of the sodium in the Mercury atmosphere is produced by photon bombardment, little of which escapes because of its relatively low velocity. A complete model of the sodium exosphere should include both photon and ion sputtering. Comparison of model predictions with data like those presented here should lead to an understanding of the relative importance of these processes.

Acknowledgements–The authors acknowledge support from the NASA Planetary Astronomy program and the National Solar Observatory at the Kitt Peak National Observatory, Arizona.

Editorial handling: A. Cochran

REFERENCES

CARLSON R. W., MATSON D. L. AND JOHNSON T. V. (1975) Electron impact ionization of Io's sodium emission cloud. *Geophys. Res. Lett.* **2**, 469–472.

GREEN D. W. E. (1992) Magnitude corrections for atmospheric extinction. *Intl. Comet Quarterly* **14**, 55–59.

HUEBNER W. F., KEADY F. J. AND LYON S. P. (1992) Solar photorates for planetary atmosphere and atmospheric pollutants. *Astrophys. Space Sci.* **195**, 1–289.

HUNTEN D. M. AND SPRAGUE A. L. (1997) Origin and character of the lunar and mercurian atmospheres. *Adv. Space Res.* **19**, 1551–1560.

HUNTEN D. M., MORGAN T. H. AND SHEMANSKY D. E. (1988) The Mercury atmosphere. In *Mercury* (eds. F. Vilas, C. R. Chapman and M. S. Matthews), pp. 562–612. Univ. Arizona Press, Tucson, Arizona, USA.

IP W-H. (1986) The sodium exosphere and magnetosphere of Mercury. *Geophys. Res. Lett.* **13**, 423–426.

IP W-H. (1990) On solar radiation-driven surface transport of sodium atoms on Mercury. *Astrophys. J.* **356**, 675–681.

KILLEN R. M. AND MORGAN T. H. (1993) Maintaining the Na atmosphere of Mercury. *Icarus* **101**, 293–312.

KILLEN R. M., POTTER A. E., FITZSIMMONS A. AND MORGAN T. H. (1999) Sodium D_2 line profiles: Clues to the temperature structure of Mercury's exosphere. *Planet. Space Sci.* **47**, 1449–1458.

KILLEN R. M., POTTER A. E., REIFF P., SARANTOS M., JACKSON B. V., HICK P. AND GILES B. (2001) Evidence for space weather at Mercury. *J. Geophys. Res.* **106**, 20 509–20 525.

MADEY T. E., YAKSHINSKIY B. V., AGEEV V. N. AND JOHNSON R. E. (1998) Desorption of alkali atoms and ions from oxide surfaces—Relevance to origins of Na and K in the atmospheres of Mercury and the Moon. *J. Geophys. Res.* **203**, 5873–5887.

MCGRATH M. A., JOHNSON R. E. AND LANZEROTTI L. J. (1986) Sputtering of sodium on the planet Mercury. *Nature* **323**, 694–696.

POTTER A. E. AND MORGAN T. H. (1997) Evidence for suprathermal sodium on Mercury. *Adv. Space Res.* **19**, 1571–1575.

POTTER A. E., KILLEN R. M. AND MORGAN T. H. (1999) Rapid changes in the sodium exosphere of Mercury. *Planet. Space Sci.* **47**, 1441–1448.

SMYTH W. H. (1986) The nature and variability of Mercury's sodium atmosphere. *Nature* **323**, 696–699.

SMYTH W. H. AND MARCONI M. L. (1995) Theoretical overview and modeling of the sodium and potassium atmospheres of Mercury. *Astrophys. J.* **441**, 839–864.

SPRAGUE A. L., KOZLOWSKI R. W. H., HUNTEN D. M., SCHNEIDER N. M., DOMINGUE D. L., WELLS W. K., SCHMITT W. AND FINK U. (1997) Distribution and abundance of sodium in Mercury's atmosphere, 1985–1988. *Icarus* **129**, 506–527.